Lanthanide(III) Complexes with 4,5-Bis(diphenylphosphinoyl)-1,2,3-triazolate and the Use of 1,10-Phenanthroline As Auxiliary Ligand

ARTICLE *in* INORGANIC CHEMISTRY · APRIL 2010

Impact Factor: 4.76 · DOI: 10.1021/ic902120e · Source: PubMed

9 AUTHORS, INCLUDING:

Marisol Correa Ascencio
Universidad Nacional Autónoma de México
1 PUBLICATION **10** CITATIONS
SEE PROFILE

Raymundo cea-olivares
Universidad Nacional Autónoma de México
108 PUBLICATIONS **1,143** CITATIONS
SEE PROFILE

Ruben ALFREDO Toscano
Instituto de Quimica, Universidad Nacional …
570 PUBLICATIONS **4,292** CITATIONS
SEE PROFILE

Verónica García-Montalvo
Universidad Nacional Autónoma de México
58 PUBLICATIONS **439** CITATIONS
SEE PROFILE

Inorganic Chemistry
Article

Inorg. Chem. **2010**, *49*, 4109–4116 **4109**
DOI: 10.1021/ic902120e

Lanthanide(III) Complexes with 4,5-Bis(diphenylphosphinoyl)-1,2,3-triazolate and the Use of 1,10-Phenanthroline As Auxiliary Ligand

Marisol Correa-Ascencio,[†] Elizabeth K. Galván-Miranda,[†] Fernando Rascón-Cruz,[†] Omar Jiménez-Sandoval,[‡] Sergio J. Jiménez-Sandoval,[‡] Raymundo Cea-Olivares,[†] Vojtech Jancik,[†] R. Alfredo Toscano,[†] and Verónica García-Montalvo*[,†]

[†]*Instituto de Química, Universidad Nacional Autónoma de México, Circuito Exterior, Ciudad Universitaria, México, D.F. 04510, México, and* [‡]*Centro de Investigación y de Estudios Avanzados del Instituto Politécnico Nacional, Unidad Querétaro, Apartado Postal 1-798, Querétaro, Qro. 76001, México*

Received October 30, 2009

New lanthanide complexes with 4,5-bis(diphenyl)phosphoranyl-1,2,3-triazolate ($\mathbf{L}^-$), $LnL_3 \cdot nH_2O$ (**1**− **8**) and $LnL_3(phen) \cdot nH_2O$ (**9**−**16**) (Ln = La, Ce, Nd, Sm, Eu, Gd, Tb, Er), have been prepared and spectroscopically characterized. The structures of $LnL_3 \cdot nH_2O$ (Ln = La, Ce, Nd, Sm and Gd) were determined by X-ray crystallography. The metal centers exhibit a distorted trigonal dodecahedron coordination environment with two symmetrically O,O-bidentate ligands and one unsymmetrically O,N- ligand attached to the metal; two oxygen atoms from neighboring dimethyl sulfoxide (DMSO) molecules complete the coordination sphere. This unsymmetrical ligand coordination behavior was also identified in solution through $^{31}P\{^1H\}$ NMR studies. Photoluminescence spectroscopy experiments in CH_2Cl_2 for both types of complexes containing Eu(III) (**6**, **14**) and Tb(III) (**7**, **15**) exhibit strong characteristic red and green emission bands for Eu(III) and Tb(III), respectively. Furthermore, $NdL_3(phen) \cdot 5H_2O$ (**11**) displays emission in the near-infrared spectral region ($^4F_{3/2} \rightarrow {}^4F_{9/2}$ at 872 nm and $^4F_{3/2} \rightarrow {}^4F_{11/2}$ at 1073 nm). The complexes containing 1,10-phenantroline exhibit higher quantum yields upon excitation at 267 nm, indicating that this auxiliary ligand promotes the luminescence of the complexes; however, luminescence lifetimes (τ) in this case are shorter than those of the $LnL_3 \cdot nH_2O$ series.

Introduction

Lanthanide coordination chemistry has been thoroughly investigated over the last 30 years[1−20] because of the interesting and functional optical, electronic, and magnetic properties trivalent lanthanides have. These particular properties make them attractive for multiple applications, such as chiral NMR shift reagents and magnetic resonance imaging contrast agents,[3] as luminescent labels for biomedical analysis,[4,5] mild reagents and catalysts in organic synthesis,[6,7] and as molecular magnetic materials.[8] For example, owing to the luminescence characteristics of several Ln^{3+} ions, they are being increasingly used as highly efficient electroluminescent devices for light emitting diodes or in the design of upconversion UV-tunable lasers,[9] luminescence probes for analysis,[10,11] as well as for recognition and chirality sensing of biological substrates.[12,13] Moreover, luminescent liquid crystals, emitting either in the visible or in the near-infrared spectral range,[14−16] and coordination polymers doped with luminescent lanthanide ions have been proposed.[17,18] Consequently, the applications of Ln(III) complexes in several important technological and medical areas, give them a prominent place in modern science.

*To whom correspondence should be addressed. E-mail: vgm@servidor.unam.mx. Phone: (+52-55) 56 22 45 05. Fax: (+52-55) 56 16 22 17.

(1) Mao, J.-G. *Coord. Chem. Rev*. **2007**, *251*, 1493.
(2) Kido, J.; Okamoto., Y. *Chem. Rev*. **2002**, *102*, 2357.
(3) Yam, V. W. W.; Lo, K. K. W. *Coord. Chem. Rev*. **1999**, *184*, 157.
(4) Bünzli, J.-C. G. *J. Alloys Compd*. **2006**, *408*−*412*, 934.
(5) Werts, M. H. V. *Sci. Prog*. **2005**, *88*, 101.
(6) Mikami, K.; Terada, M.; Matsuzawa, H. *Angew. Chem., Int. Ed*. **2002**, *41*, 3554.
(7) Aspinall, H. C. *Chem. Rev*. **2002**, *102*, 1807.
(8) Ishikawa, N.; Sugita, M.; Ishikawa, T.; Koshihara, S.; Kaizu, Y. *J. Am. Chem. Soc*. **2003**, *125*, 8694.
(9) Auzel, F. *Chem. Rev*. **2004**, *104*, 139.
(10) Parker, D. *Coord. Chem. Rev*. **2000**, *205*, 109.
(11) Comby, S.; Bünzli, J.-C. G. Lanthanide Near-Infrared Luminescence in Molecular Probes and Devices. In *Handbook on the Physics and Chemistry of Rare Earths*; Gschneidner, K. A., Jr., Bünzli, J.-C. G., Pecharsky, V. K., Eds.; Elsevier Science B.V.: Amsterdam, 2007.
(12) *Metal Ions in Biological Systems: The Lanthanides and their Interrelations with Biosystems*; Sigel, A., Sigel, H, Eds.; Frontis Media S.A., Marcel Dekker.Inc: NewYork, 2003.
(13) Tsukube, H.; Shinoda, S.; Tamiaki, H. *Coord. Chem. Rev*. **2002**, *226*, 227.
(14) Binnemans, K.; Görller-Walrand, C. *Chem. Rev*. **2002**, *102*, 2303.
(15) Suárez, S.; Mamula, O.; Imbert, D.; Piguet, C.; Bünzli, J.-C. G. *Chem. Commun*. **2003**, 1226.
(16) Van Deun, R.; Moors, D.; De Fre, B.; Binnemans, K. *J. Mater. Chem*. **2003**, *13*, 1520.
(17) Liu, W.; Jiao, T.; Liu, Q.; Minyu, T.; Wang, H.; Wang, L. *J. Am. Chem. Soc*. **2004**, *126*, 2280.
(18) Bünzli, J.-C. G.; Piguet, C. *Chem. Rev*. **2002**, *102*, 1897.
(19) Kim, H. J.; Lee, J. E.; Kim, Y. S.; Park, N. G. *Opt. Mater*. **2002**, *21*, 181.
(20) Mato-Iglesias, M.; Rodríguez-Blas, T.; Platas-Iglesias, C.; Starck, M.; Kadjane, P.; Ziessel, R.; Charbonniere, L. *Inorg. Chem*. **2009**, *48*, 1507.

Published on Web 04/09/2010

On the other hand, compounds of general formula $R_2P(O)$-X-$P(O)R_2$ have been widely used as chelating ligands in coordination chemistry for at least two decades.[21] Some of these P(O)-X-P(O) ligands with X = NH,[22−24] HNRNH,[25] CH_2,[26] CH_2CH_2,[27] and some mono- and multidentate ligands containing the $Ph_2P(O)$ moiety[1,28−31] have been employed as potential sensitizing ligands for lanthanide ions in recent years. Furthermore, many dialkyl-, diphenyl-, or diphenoxyphosphinic substrates are commercially available, which makes many of the ligand synthetic routes conceivable and attractive. On this basis and considering the lanthanides preference for hard donors atoms, P(O)-X-P(O) bidentate ligands appear to be quite suitable to coordinate lanthanides. Recently, we turned our attention to the triazole based phosphoranyl ligand 4,5-bis(diphenyl)phosphinoyl-1,2,3-triazole (**L** = 4,5-$(Ph_2P(O))_2$Tz; Tz = triazole),[32] which is a P(O)-X-P(O) bidentate ligand that holds a variety of potential coordination sites, as it is observed in the five- and seven-membered chelate rings that exhibit the reported O,N- and O, O-bidentate coordination mode of the anionic ligands[32] and the E,N,N-tridentate bimetallic coordination observed in dimers of dimethylaluminum and -gallium, $[4,5\text{-}(P(E)Ph_2)_2(\mu\text{-tz})]MMe_2\}_2$ (M = Al, Ga; E = O, S), and lithium and sodium compounds, $[4,5\text{-}(P(E)Ph_2)_2(\mu\text{-tz})]\text{-}M(solvent)_n\}_2$ (M = Li, Na; E = S or Se).[33]

In this work, we report the synthesis, characterization, and a comparative study of two lanthanide complexes series: $LnL_3\cdot nH_2O$ (**1**− **8**) and $LnL_3(phen)\cdot nH_2O$ (**9**−**16**) (Ln = La, Ce, Nd, Sm, Eu, Gd, Tb, and Er), with the anionic oxygen-based ligand ($\mathbf{L}^-$). After determining the X-ray diffraction structures of $[LaL_3(DMSO)_2]\cdot 3/2DMSO$, $[CeL_3(DMSO)_2]\cdot 2H_2O$, $[NdL_3(DMSO)_2]\cdot 2H_2O$, $[SmL_3(DMSO)_2]\cdot 2H_2O$, $[GdL_3(DMSO)_2]\cdot 2H_2O/MeOH$, we decided to synthesize the $LnL_3(phen)\cdot nH_2O$ series (**9**− **16**) using 1,10-phenanthroline (phen) as an auxiliary ligand, to increase the luminescence properties and to exclude coordinated water or solvent molecules that may provoke the quenching of this. Photoluminescence spectroscopy results in CH_2Cl_2 for the $LnL_3\cdot nH_2O$ and $LnL_3(phen)\cdot nH_2O$ complexes with Ln = Eu(III) (**6**, **14**) and Tb(III) (**7**, **15**), and for $NdL_3(phen)\cdot nH_2O$ (**11**) are discussed. The X-ray structures exhibit a distorted trigonal dodecahedron coordination environment with two symmetrically O,O-bidentate ligands and one unsymmetrically O,N-bidentate ligand attached to the metal, in addition to two oxygen atoms from DMSO molecules that complete the coordination sphere. The unsymmetrical ligand coordination behavior was also observed in solution through $^{31}P\{^1H\}$ NMR studies.

Experimental Section

General Information. All chemicals were purchased from Sigma-Aldrich and were used without further purification. The preparation of **L** was performed following the method described in the literature.[32] The potassium salt (KL) was obtained from the reaction of **L** with potassium *tert*-butoxide in ethanol. Melting points were determined with a Mel-Temp II instrument and are uncorrected. FAB+ Mass spectra were measured on a 3-nitrobenzyl alcohol support in the positive ion mode on a Jeol JMS-SX102A spectrometer and ESI-Mass spectra were obtained on a Bruker microTOF II instrument (in CH_3CN). FT-IR spectra were recorded on a Bruker Tensor 27 spectrometer in the 3500−210 cm^{-1} range as CsI pellets. Raman spectroscopic data were recorded at room temperature in a Dilor LabRam micro spectrometer equipped with a confocal microscope, using the 632.8 nm line of a He−Ne laser; a 50× microscope objective was used, which produced a laser spot of ∼2 μm in diameter. Absorption spectra were recorded on a Cary-50 (Varian) system. Steady-state and time-resolved emission spectra were recorded on a Cary Eclipse spectrophotometer (Varian) upon excitation at 267 nm. The delay time was 0.01 ms for period of 50 ms. The emission quantum yields (Φ_F) of **6**, **7**, **11**, **14**, **15** were calculated by $\Phi_x = (A_s/A_x)(F_x/F_s)(n_x/n_s)^2\Phi_s$ using *p*-Terphenyl in methanol as standard (Φ_F = 0.85). The subscripts s and *x* denote the reference standard and the sample solution, respectively; *n*, *F*, *A*, and Φ are the refractive index of the solvents, the integrated intensity, the absorbance at the excitation wavelength, and the luminescence quantum yield, respectively. All measurements were performed at (20 ± 0.5 °C) in 1 cm quartz cells with HPLC quality solvent (CH_2Cl_2). ^1H (300 MHz) and ^{31}P NMR (121 MHz) were recorded on a Jeol Eclipse 300 or a Bruker Advance 300 spectrometer, at 20 °C; chemical shifts were referenced to tetramethylsilane (^1H) and H_3PO_4 85% (^{31}P). Elemental analyses were performed on an Exeter Analytical CE-440 CHN Elemental Analyzer. Magnetic susceptibilities were measured at room temperature using a Sherwood Scientific Ltd. balance standardized with $HgCo(NCS)_4$; diamagnetic corrections were estimated from Pascal's constants. Thermogravimetric analyses (TGA) were performed on a Mettler-Toledo TGA/SDTA851 instrument, in a nitrogen atmosphere with a 50 cm^3 min^{-1} flow rate; the heating rate was 10 °C min^{-1}.

Preparation of $LnL_3\cdot nH_2O$ [Ln^{3+} = La (1), Ce(2), Nd(3), Sm(4), Gd(5), Eu(6), Tb(7), Er(8)]. The synthetic method consisted on dispersing 3 mol equiv of KL in 10 mL of tetrahydrofuran (THF); to this solution, 1 equiv of the corresponding $LnCl_3\cdot nH_2O$ previously dissolved in the minimum quantity of water was then added. The resulting clear solution was stirred until a fine precipitate appeared and then concentrated by vacuum distillation. The solid product was collected by filtration and washed with water.

$LaL_3\cdot 3H_2O$ (1). 100 mg (0.197 mmol) of KL, 24.5 mg (0.066 mmol) of $LaCl_3\cdot 6H_2O$. Yield 90 mg (88.76%). Mp 379 °C (dec.). *Anal.* Calcd for $C_{78}H_{60}LaN_9O_6P_6\cdot 3H_2O$: C, 58.62; H, 4.16; N, 7.89. Found: C, 58.59; H, 4.13; N, 7.86%. ESI $^+$-MS (MeCN, *m*/*z*): 1578.25 $[M+H_2O]^+$. FAB^+-MS (*m*/*z*): 1543 (M^+, 3%). IR (CsI, cm^{-1}): 1155, 1187 (ν_{PQ}), 358 ($\nu_{La\text{-}X}$, X = O,N). UV−vis (10^{-5} *M*, CH_2Cl_2, nm/ ε M^{-1} cm^{-1}): λ_1 267 (14880), λ_2 274 (11320). ^1H NMR (DMSO-d_6, ppm): δ 7.0 (br *s*, 24H, *m*-H Ph), 7.3 (br *s*, 12H, *p*-H Ph), 7.5 (br *s*, 24H, *o*-H Ph); ^{31}P NMR (DMSO-d_6, ppm): δ 17.1, 25.9. μ_{eff} (20 °C) = 0 μ_B.

(21) Silvestru, C.; Drake, J. E. *Coord. Chem. Rev.* **2001**, *223*, 117.
(22) Christou, V.; Salata, O. V.; Ly, Q.; Capecchi, S.; Bailey, N. J.; Cowley, A.; Chippindale, A. M. *Synth. Met.* **2000**, *111*, 7.
(23) Bassett, A.; Van Deun, R.; Nockermann, P.; Glover, P. B.; Kariuki, M. B.; Van Hecke, K.; Van Meervelt, L.; Pikramenou, Z. *Inorg. Chem.* **2005**, *44*, 6140.
(24) Pietraszkiewicz, M.; Karpiuk, J.; Staniszewski, K. *J. Alloys Compd.* **2002**, *341*, 267.
(25) Kim, Y. K.; Livinghouse, T.; Horino, Y. *J. Am. Chem. Soc.* **2003**, *125*, 9560.
(26) Lees, A. M. J.; Platt, A. W. G. *Inorg. Chem.* **2003**, *42*, 4673.
(27) Spichal, Z.; Necas, M.; Pinkas, J.; Novosad, J. *Inorg. Chem.* **2004**, *43*, 2776.
(28) Paine, R. T.; Bond, E. M.; Parveen, S.; Donhart, N.; Duesler, E. N.; Smith, K. A.; Nöth, H. *Inorg. Chem.* **2000**, *41*, 444.
(29) Hill, N. J.; Levason, W.; Popham, M. C.; Reid, G.; Webster, M. *Polyhedron* **2002**, *21*, 445.
(30) Gan, X.; Rapko, B M.; Duesler, E. N.; Binyamin, I.; Paine, R. T.; Hay, B. P. *Polyhedron* **2005**, *24*, 469.
(31) Levason, W.; Newman, E. H.; Webster, M. *Polyhedron* **2000**, *19*, 2697.
(32) Liable-Sands, L. M.; Trofimenko, S. *Angew. Chem., Int. Ed.* **2000**, *39*, 3321.
(33) Moya-Cabrera, M.; Jancik, V.; Castro, R. A.; Herbst-Irmer, R.; Roesky, H. W. *Inorg. Chem.* **2006**, *45*, 5167.

$CeL_3 \cdot 6H_2O$ (2). 100 mg (0.197 mmol) of KL, 24.5 mg (0.066 mmol) of $CeCl_3 \cdot 6H_2O$. Yield 90 mg (88.24%). Mp 383 °C (dec). *Anal.* Calcd for $C_{78}H_{60}CeN_9O_6P_6 \cdot 6H_2O$: C, 56.66; H, 4.39; N, 7.62. Found: C, 56.64; H, 4.49; N, 7.61. ESI$^+$-MS (MeCN, *m*/*z*): 1545.17 $[M+H]^+$, 1579.23 $[M + 2H_2O - H]^+$. FAB$^+$-MS (*m*/*z*): 1545 ($[M+H]^+$, 76%). IR (CsI, cm^{-1}): 1143, 1157 (ν_{PO}), 359 ($\nu_{Ce\text{-}X}$, X = O,N). UV−vis (10^{-5} *M*, CH_2Cl_2, nm/ ε M^{-1} cm^{-1}): λ_1 267 (11930), λ_2 274 (9370). ^{1}H NMR (DMSO-d_6, ppm): δ 6.7 (br *s*, 24H, *m*-H Ph), 6.9 (br *s*, 12H, *p*-H Ph), 7.2 (br *s*, 24H, *o*-H Ph); ^{31}P NMR (DMSO-d_6, ppm): δ 17.5, 49.3. μ_{eff} (20 °C) = 3.39 μ_B.

$NdL_3 \cdot 6H_2O$ (3). 100 mg (0.197 mmol) of KL, 23 mg (0.066 mmol) of $NdCl_3 \cdot 6H_2O$. Yield 92 mg, (89.98%). Mp 390 °C (dec.). *Anal.* Calcd for $C_{78}H_{60}NdN_9O_6P_6 \cdot 6H_2O$: C, 56.52; H, 4.38; N, 7.61. Found: C, 56.55; H, 4.35; N, 7.60. ESI$^+$-MS (MeCN, *m*/*z*): 1549.19 $[M+H]^+$, 1583.25 $[M + 2H_2O - H]^+$. FAB$^+$-MS (*m*/*z*): 1549 ($[M+H]^+$, 11%). IR (CsI, cm^{-1}): 1145, 1159 (ν_{PO}), 364 ($\nu_{Nd\text{-}X}$, X = O,N) .UV−vis (10^{-5} *M*, CH_2Cl_2, nm/ ε M^{-1} cm^{-1}): λ_1 267 (12600), λ_2 274 (10040). ^{1}H NMR (DMSO-d_6, ppm): δ 6.8 (br *s*, 24H, Ph), 7.2 (br *s*, 36H, Ph); ^{31}P NMR (DMSO-d_6, ppm): δ 17.4, 104.6. μ_{eff} (20 °C) = 4.29 μ_B.

$SmL_3 \cdot 7H_2O$ (4). 100 mg (0.197 mmol) of KL, 24 mg (0.066 mmol) of $SmCl_3 \cdot 6H_2O$. Yield 80 mg (77.94%). Mp 394 °C (dec). *Anal.* Calcd for $C_{78}H_{60}N_9O_6P_6Sm \cdot 7H_2O$: C, 55.71; H, 4.44; N, 7.50. Found: C, 55.76; H, 4.40; N, 7.51. ESI$^+$-MS (MeCN, *m*/*z*): 1559.19 $[M+H]^+$, 1593.26 $[M + 2H_2O - H]^+$. FAB$^+$-MS (*m*/*z*): 1559 ($[M+H]^+$, 7%). IR (CsI, cm^{-1}): 1134, 1159 (ν_{PO}), 362 ($\nu_{Sm\text{-}X}$, X = O,N). UV−vis (10^{-5} *M*, CH_2Cl_2, nm/ ε M^{-1} cm^{-1}): λ_1 267 (20770), λ_2 274 (27260). ^{1}H NMR (DMSO-d_6, ppm): δ 7.0 (br *s*, 24H, *m*-H Ph), 7.3 (br *s*, 12H, *p*-H Ph), 7.4 (br *s*, 24H, *o*-H Ph); ^{31}P NMR (DMSO-d_6, ppm): δ 17.4, 26.2. μ_{eff} (20 °C) = 2.41 μ_B.

$GdL_3 \cdot 4H_2O$ (5). 100 mg (0.197 mmol) of KL, 24.5 mg (0.066 mmol) of $GdCl_3 \cdot 6H_2O$. Yield 86 mg (83.20%). Mp 399 °C (dec). *Anal.* Calcd for $C_{78}H_{60}GdN_9O_6P_6 \cdot 4H_2O$: C, 57.32; H, 4.19; N, 7.71. Found: C, 57.29; H, 4.21; N, 7.70. ESI$^+$-MS (MeCN, *m*/*z*): 1563.17 $[M+H]^+$, 1585.15 $[M+1.3H_2O]^+$. FAB$^+$-MS (*m*/*z*) 1563 ($[M+H]^+$, 45%). IR (CsI, cm^{-1}): 1136, 1145 (ν_{PO}), 362 ($\nu_{Gd\text{-}X}$, X = O,N). UV−vis (10^{-5} *M*, CH_2Cl_2, nm/ ε M^{-1} cm^{-1}): λ_1 267 (25820), λ_2 274 (20640). ^{1}H NMR (DMSO-d_6, ppm): δ 7.5 (br *s*, 60H, Ph). μ_{eff} (20 °C) = 7.87 μ_B.

$EuL_3 \cdot 6H_2O$ (6). 50 mg (0.099 mmol) of KL, 12.1 mg (0.033 mmol) of $EuCl_3 \cdot 6H_2O$. Yield 35 mg (68.87%). Mp 392 °C (dec). *Anal.* Calcd for $C_{78}H_{60}EuN_9O_6P_6 \cdot 6H_2O$: C, 56.26; H, 4.36; N, 7.57. Found: C, 56.26; H, 4.38; N, 7.58. ESI$^+$-MS (MeCN, *m*/*z*): 1558.17 $[M+H]^+$, 1592.24 $[M + 2H_2O - H]^+$. FAB$^+$-MS (*m*/*z*) 1558 ($[M+H]^+$, 78%). IR (CsI, cm^{-1}): 1143, 1162 (ν_{PO}), 393 ($\nu_{Eu\text{-}X}$, X = O,N). UV−vis (10^{-5} *M*, CH_2Cl_2, nm/ ε M^{-1} cm^{-1}): λ_1 267 (29450), λ_2 274 (21900). ^{1}H NMR (DMSO-d_6, ppm): δ 7.2 (br *s*, 24H, *m*-H Ph), 7.5 (br *s*, 12H, *p*-H Ph), 7.9 (br *s*, 24H, *o*-H Ph); ^{31}P NMR (DMSO-d_6, ppm): δ 18.0, −69.6. μ_{eff} (20 °C) = 4.02 μ_B.

$TbL_3 \cdot 4H_2O$ (7). 50 mg (0.099 mmol) of KL, 12.1 mg (0.033 mmol) of $TbCl_3 \cdot 6H_2O$. Yield 40 mg (77.55%). Mp 412 °C (dec). *Anal.* Calcd for $C_{78}H_{60}N_9O_6P_6Tb \cdot 4H_2O$: C, 57.26; H, 4.19; N, 7.70. Found: C, 57.24; H, 4.23; N, 7.71. ESI$^+$-MS (MeCN, *m*/*z*): 1564.18 $[M+H]^+$, 1598.25 $[M + 2H_2O - H]^+$. FAB$^+$-MS (*m*/*z*): 1564 ($[M+H]^+$, 8%). IR (CsI, cm^{-1}): 1128, 1188 (ν_{PO}), 427 ($\nu_{Tb\text{-}X}$, X = O,N). UV−vis (10^{-5} *M*, CH_2Cl_2, nm/ ε M^{-1} cm^{-1}): λ_1 267 (24180), λ_2 274 (32280). ^{31}P NMR (DMSO-d_6, ppm): δ 17.7, −160.1. μ_{eff} (20 °C) = 6.89 μ_B.

$ErL_3 \cdot 2H_2O$ (8). 100 mg (0.197 mmol) of KL, 25.2 mg (0.066 mmol) of $ErCl_3 \cdot 6H_2O$. Yield 87 mg (83.84%). Mp 401 °C (dec). *Anal.* Calcd for $C_{78}H_{60}ErN_9O_6P_6 \cdot 2H_2O$: C, 58.24; H, 4.01; N, 7.84. Found: C, 58.21; H, 4.05; N, 7.80. ESI$^+$-MS (MeCN, *m*/*z*): 1573.20 $[M+H]^+$, 1607.28 $[M + 2H_2O - H]^+$. FAB$^+$-MS (*m*/*z*): 1573 ($[M+H]^+$, 6%). IR (CsI, cm^{-1}): 1140, 1148 (ν_{PO}), 364 ($\nu_{Er\text{-}X}$, X = O,N). UV−vis (10^{-5} *M*, CH_2Cl_2, nm/ ε M^{-1} cm^{-1}): λ_1 267 (26190), λ_2 274 (24770). μ_{eff} (20 °C) = 8.62 μ_B.

Preparation of $LnL_3(phen) \cdot nH_2O$ [Ln^{3+} = La (9), Ce (10), Nd (11), Sm (12), Gd(13), Eu(14), Tb(15), Er(16)]. The first stage of the synthesis of LnL_3(phen) was performed as described above. One molar equivalent of 1,10-phenanthroline (phen) was added to the clear solution of KL and $LnCl_3 \cdot nH_2O$, before any fine precipitate appeared. The solvent was removed by vacuum distillation to dryness and then water was added. The solid was collected by filtration.

$LaL_3(phen) \cdot 3H_2O$ (9). 50 mg (0.099 mmol) of KL, 12.3 mg (0.033 mmol) of $LaCl_3 \cdot 6H_2O$, 6 mg (0.033 mmol) of Phen. Yield 46.7 mg (79.69%). Mp 400 °C (dec). *Anal* Calcd for $C_{90}H_{68}LaN_{11}O_6P_6 \cdot 3H_2O$: C, 60.78; H, 4.19; N, 8.66 Found: C, 60.74; H, 4.24; N, 8.67. ESI$^+$-MS (MeCN,*m*/*z*): 1763.26 $[M+2H_2O+3H]^+$, 1725.25 $[M+ H]^+$, 1582.13 $[M\text{-phen}+2H_2O+2H]^+$, 1255.14 $[M - L+ H]^+$. FAB$^+$-MS (*m*/*z*): 1724 (M^+, 3%). IR (CsI, cm^{-1}): 1149, 1156 (ν_{PO}), 405 ($\nu_{La\text{-}X}$, X = O,N). UV−vis (10^{-5} *M*, CH_2Cl_2, nm/ ε M^{-1} cm^{-1}) λ_1 267 (95860), λ_2 274 (96750), λ_2 294 (35270). ^{1}H NMR (DMSO-d_6, ppm): δ 7.1 (br *s*, 24H, *m*-H Ph), 7.4 (br *s*, 12H, *p*-H Ph), 7.6 (br *s*, 24H, *o*-H Ph), 7.8 (m, 2H, $H_{3,8}$ phen), 8.0 (s, 2H, $H_{5,6}$ phen), 8.5 (d, $^1J_{H-H}$ = 8.28 Hz, 2H, $H_{4,7}$ phen), 9.1 (s, 2H, $H_{2,9}$ phen); ^{31}P NMR (DMSO-d_6, ppm): δ 18.7, 26.5. μ_{eff} (20 °C) = 0 μ_B.

$CeL_3(phen) \cdot 5H_2O$ (10). 50 mg (0.099 mmol) of KL, 12.3 mg (0.033 mmol) of $CeCl_3 \cdot 6H_2O$, 6 mg (0.033 mmol) of Phen. Yield 39.9 mg (70.09%). Mp 366 °C (dec). *Anal.* Calcd for $C_{90}H_{68}CeN_{11}O_6P_6 \cdot 5H_2O$: C, 59.54; H, 4.33; N, 8.49. Found: C, 59.51; H, 4.30; N, 8.5. ESI$^+$-MS (MeCN,*m*/*z*): 1764.23 $[M+2H_2O+3H]^+$, 1726.27 $[M+H]^+$, 1583.15 $[M\text{-phen}+2H_2O+2H]^+$, 1256.16 $[M - L]^+$. FAB$^+$-MS (*m*/*z*): 1724 ($[M - H]^+$, 2%). IR (CsI, cm^{-1}): 1147,1185 (ν_{PO}), 425 ($\nu_{Ce\text{-}X}$, X = O,N). UV−vis (10^{-5} *M*, CH_2Cl_2, nm/ ε M^{-1} cm^{-1}): λ_1 267 (32130), λ_2 274 (36450), λ_3 294 (11910). ^{1}H NMR (DMSO-d_6, ppm): δ 6.8 (br *s*, 36H, Ph), 7.1 (br *s*, 24H, *o*-H Ph), 7.8 (m, 2H, $H_{3,8}$ phen), 9.1 (s, 2H, $H_{2,9}$ phen), 8.0 (s, 2H, $H_{5,6}$ phen), 8.5 (d, $^1J_{H-H}$ = 7.41 Hz, 2H, $H_{4,7}$ phen); ^{31}P NMR (DMSO-d_6, ppm): δ 17.5, 50.0. μ_{eff} (20 °C) = 3.86 μ_B.

$NdL_3(phen) \cdot 5H_2O$ (11). 50 mg (0.099 mmol) of KL, 11.8 mg (0.033 mmol) of $NdCl_3 \cdot 6H_2O$, 6 mg (0.033 mmol) of Phen. Yield 30.5 mg, (53.63%). Mp 383 °C (dec). *Anal.* Calcd for $C_{90}H_{68}NdN_{11}O_6P_6 \cdot 5H_2O$: C, 59.40; H, 4.32; N, 8.47. Found: C, 59.39; H, 4.30; N, 8.47. ESI$^+$−MS (MeCN,*m*/*z*): 1583.24 $[M\text{-phen}+2H_2O]^+$. FAB$^+$-MS (*m*/*z*): 1729 ($[M+H]^+$, 2%). IR (CsI, cm^{-1}): 1150, 1171 (ν_{PO}), 397 ($\nu_{Nd\text{-}X}$, X = O,N). UV−vis (10^{-5} *M*, CH_2Cl_2, nm/ε M^{-1} cm^{-1}): λ_1 267 (74780), λ_2 274 (78840), λ_3 294 (27820). ^{1}H NMR (DMSO-d_6, ppm): δ 6.8 (br *s*, 24H, *m*-H Ph), 6.9 (br *s*, 12H, *p*-H Ph), 7.2 (br *s*, 24H, *o*-H Ph), 7.8 (m, 2H, $H_{3,8}$ phen), 8.0 (s, 2H, $H_{5,6}$ phen), 8.5 (d, $^1J_{H-H}$ = 7.2 Hz, 2H, $H_{4,7}$ phen), 9.1 (s, 2H, $H_{2,9}$ phen); ^{31}P NMR (DMSO-d_6, ppm): δ 17.5, 100.1. μ_{eff} (20 °C) = 4.62 μ_B.

$SmL_3(phen) \cdot 5H_2O$ (12). 50 mg (0.099 mmol) of KL, 12.05 mg (0.033 mmol) of $SmCl_3 \cdot 6H_2O$, 6 mg (0.033 mmol) of Phen. Yield 35.5 mg (61.82%). Mp 386 °C (dec). *Anal.* Calcd for $C_{90}H_{68}N_{11}O_6P_6Sm \cdot 5H_2O$: C, 59.20; H, 4.31; N, 8.44. Found: C, 59.17; H, 4.28; N, 8.45. ESI$^+$-MS (MeCN,*m*/*z*): 1773.20 $[M + 2H_2O - H]^+$, 1756.22 $[M+H_2O]^+$, 1739.25 $[M+H]^+$, 1597.14 $[M\text{-phen}+2H_2O+3H]^+$. FAB$^+$-MS (*m*/*z*): 1738 ($M^+$, 3%). IR (CsI, cm^{-1}): 1151, 1187 (ν_{PO}). 425 ($\nu_{Sm\text{-}X}$, X = O,N). UV−vis (10^{-5} *M*, CH_2Cl_2, nm/ ε M^{-1} cm^{-1}): λ_1 267 (45130), λ_2 274 (42180), λ_3 294 (13410). ^{1}H NMR (DMSO-d_6, ppm): δ 7.0 (br *s*, 24H, *m*-H Ph), 7.3 (br *s*, 12H, *p*-H Ph), 7.4 (br *s*, 24H, *o*-H Ph), 7.8 (m, 2H, $H_{3,8}$ phen), 8.0 (s, 2H, $H_{5,6}$ phen), 8.5 (d, $^1J_{H-H}$ = 7.8 Hz, 2H, $H_{4,7}$ phen), 9.1 (s, 2H, $H_{2,9}$ phen); ^{31}P NMR (DMSO-d_6, ppm): δ 17.5, 26.0. μ_{eff} (20 °C) = 1.72 μ_B.

$GdL_3(phen) \cdot 3H_2O$ (13). 50 mg (0.099 mmol) of KL, 12.2 mg (0.033 mmol) of $GdCl_3 \cdot 6H_2O$, 6 mg (0.033 mmol) of Phen. Yield 25.6 mg (44.53%). M. p.391 °C (dec). *Anal.* Calcd for $C_{90}H_{68}GdN_{11}O_6P_6 \cdot 3H_2O$: C, 60.16; H, 4.15; N 8.58. Found: C, 60.19; H, 4.20; N, 8.6. ESI$^+$-MS (MeCN,*m*/*z*): 1781.19 $[M+2H_2O+4H]^+$, 1743.23 $[M+2H]^+$, 1601.12 $[M\text{-phen}+2H_2O+3H]^+$. FAB$^+$-MS (*m*/*z*): 1742 ($[M+H]^+$, 5%). IR (CsI, cm^{-1}): 1153, 1185 (ν_{PO}), 424 ($\nu_{Gd\text{-}X}$, X = O,N). UV−vis (10^{-5} *M*, CH_2Cl_2, nm/ ε M^{-1} cm^{-1}): λ_1 267 (69720), λ_2 274 (59400), λ_3 294 (16830). ^{1}H NMR (DMSO-d_6, ppm): δ 7.3 (br *s*, 60H, Ph), 7.8 (m, 2H, $H_{3,8}$ phen),

Table 1. Selected Crystallographic Data for Compounds $[LaL_3(DMSO)_2]\cdot 3/2DMSO$, $[CeL_3(DMSO)_2]\cdot 2H_2O$, $[NdL_3(DMSO)_2]\cdot 2H_2O$, $[SmL_3(DMSO)_2]\cdot 2H_2O$, $[GdL_3(DMSO)_2]\cdot 2H_2O/MeOH$

	$[LaL_3(DMSO)_2]\cdot 3/2DMSO$	$[CeL_3(DMSO)_2]\cdot 2H_2O$	$[NdL_3(DMSO)_2]\cdot 2H_2O$	$[SmL_3(DMSO)_2]\cdot 2H_2O$	$[GdL_3(DMSO)_2]\cdot 2H_2O/MeOH$
formula (sum)	$C_{169}H_{159}La_2N_{18}O_{19}P_{12}S_7$	$C_{82}H_{76}CeN_9O_{10}P_6S_2$	$C_{82}H_{76}N_9NdO_{10}P_6S_2$	$C_{82}H_{76}N_9O_{10}P_6S_2Sm$	$C_{82}H_{76}GdN_9O_{10}P_6S_2$
M [g/mol]	1810.05	1737.58	1741.70	1747.81	1769.77
crystal size (mm)	0.206 × 0.086 × 0.044	0.302 × 0.124 × 0.086	0.216 × 0.052 × 0.036	0.224 × 0.082 × 0.054	0.362 × 0.078 × 0.062
crystal system	triclinic	monoclinic	monoclinic	monoclinic	monoclinic
space group	$P\bar{1}$	$P2_1$	$P2_1$	$P2_1$	$P2_1$
ρ_{calc}(Mg m^{-3})	1.407	1.429	1.435	1.445	1.457
Z	2	2	2	2	2
a (Å)	11.850(1)	12.179(3)	12.230(5)	12.197(3)	12.110(3)
b (Å)	13.642(2)	21.086(4)	21.105(8)	21.015(4)	21.141(4)
c (Å)	27.146(3)	16.496(4)	16.403(6)	16.447(4)	16.583(3)
α (deg)	98.769(2)	90	90	90	90
β (deg)	99.367(2)	107.62(4)	107.81(2)	107.64(4)	108.13(3)
γ (deg)	92.057(2)	90	90	90	90
V (Å^3)	4270.9(9)	4037.5(16)	4031(3)	4017.5(16)	4034.8(15)
μ (mm^{-1})	0.760	0.798	0.879	0.967	1.058
F(000)	1857	1782	1786	1790	1811
abs. correction method	"multiscan"	"multiscan"	"multiscan"	"multiscan"	"multiscan"
min.,max. transmission	0.8601, 0.9695	0.8472, 0.9408	0.8683, 0.9720	0.8665, 0.9535	0.7007, 0.9373
reflections collected	35310	33348	31379	32935	28234
unique reflections R_{int}	15634; 0.0986	14217; 0.0697	14731; 0.0891	14155; 0.0530	13906; 0.0402
$R1$, $wR2$ [$I > 2\sigma(I)$]	0.0741; 0.1335	0.0570; 0.1036	0.0650; 0.1090	0.0545; 0.1070	0.0510; 0.1064
$R1$, $wR2$ (all data)	0.01297; 0.1541	0.0697; 0.1088	0.0952; 0.1206	0.0645; 0.1110	0.0591, 0.1100
GoF	1.016	1.012	0.992	1.036	1.009
Flack parameter		0.348(10)	0.462(11)	0.403(9)	0.195(8)
large residuals (e Å^{-3})	0.797 /−1.147	1.5010/−0.529	1.263/−0.932	1.464 /−1.430	1.383/−0.982

7.9 (s, 2H, $H_{5,6}$ phen), 8.5 (s, $H_{4,7}$ phen), 9.1 (s, 2H, $H_{2,9}$ phen). μ_{eff} (20 °C) = 9.4 μ_B.

EuL_3(phen)·$2H_2O$ (14). 50 mg (0.099 mmol) of KL, 12.05 mg (0.033 mmol) of $EuCl_3\cdot 6H_2O$, 6 mg (0.033 mmol) of Phen. Yield 42.3 mg (73.95%). Mp 388 °C (dec). *Anal.* Calcd for $C_{90}H_{68}EuN_{11}O_6P_6\cdot 2H_2O$: C, 60.95; H, 4.09; N, 8.69. Found: C, 60.96; H, 4.13; N, 8.65. ESI$^+$-MS (MeCN,*m*/*z*): 1776.24 $[M+2H_2O+3H]^+$, 1738.28 $[M+H]^+$, 1592.27 $([M\text{-phen}+2H_2O-H]^+$, 1558.22 $([M\text{-phen}+H]^+$, 1269.18 $[M-L]^+$. FAB$^+$-MS (*m*/*z*): 1738 ($[M+H]^+$, 2%). IR (CsI, cm^{-1}): 1151, 1186 (ν_{PO}). UV−vis (10^{-5} *M*, CH_2Cl_2, nm/ ε M^{-1} cm^{-1}): λ_1 267 (105710), λ_2 274 (93720), λ_3 294 (26870). ^{1}H NMR (DMSO-d_6, ppm): δ 7.2 (br *s*, 24H, *m*-H Ph), 7.5 (br *s*, 12H, *p*-H Ph), 7.7 (br *s*, 24H, *o*-H Ph), 7.8 (m, 2H, $H_{3,8}$ phen), 8.0 (s, 2H, $H_{5,6}$ phen), 8.5 (d, $^1J_{H-H}$ = 7.95 Hz, 2H, $H_{4,7}$ phen), 9.1 (d, $^1J_{H-H}$ = 4.4 Hz, 2H, $H_{2,9}$ phen); ^{31}P NMR (DMSO-d_6, ppm): δ17.4, −83.0. μ_{eff} (20 °C) = 4.12 μ_B.

TbL_3(phen)·$4H_2O$ (15). 50 mg (0.099 mmol) of KL, 12.1 mg (0.033 mmol) of $TbCl_3\cdot 6H_2O$, 6 mg (0.033 mmol) of Phen. Yield 33.2 mg (57.68%). Mp 387 °C (dec). *Anal.* Calcd for $C_{90}H_{68}N_{11}O_6P_6Tb\cdot 4H_2O$: C, 59.51; H, 4.22; N, 8.48. Found: C, 59.54; H, 4.20; N, 8.45. ESI$^+$-MS (MeCN,*m*/*z*): 1783.20 $[M+2H_2O+3H]^+$, 1745.23 $[M+H]^+$, 1602.12 $([M\text{-phen}+2H_2O-H]^+$, 1564.17 $[M\text{-phen}]^+$, 1275.14 $[M-L-H]^+$. FAB$^+$-MS (*m*/*z*): 1745 ($[M+H]^+$, 3%). IR (CsI, cm^{-1}): 1152, 1187 (ν_{PO}), 422 ($\nu_{Tb\text{-}X}$, X = O,N). UV−vis (10^{-5} *M*, CH_2Cl_2, nm/ ε M^{-1} cm^{-1}): λ_1 267 (66510), λ_2 274 (57510), λ_3 294 (16350). ^{31}P NMR (DMSO-d_6, ppm): δ17.2, −153.4. μ_{eff} (20 °C) = 8.35 μ_B.

ErL_3(phen)·$7H_2O$ (16). 50 mg (0.099 mmol) of KL, 12.5 mg (0.033 mmol) of $ErCl_3\cdot 6H_2O$, 6 mg (0.033 mmol) of Phen. Yield 26.5 mg (45.75%). Mp 339 °C (dec). *Anal.* Calcd for $C_{90}H_{68}ErN_{11}O_6P_6\cdot 7H_2O$: C, 57.54; H, 4.40; N, 8.20. Found: C, 57.52; H, 4.38; N, 8.21. ESI$^+$-MS (MeCN, *m*/*z*): 1791.31 $[M+2H_2O+2H]^+$, 1607.23 $[M\text{-phen}+2H_2O-H]^+$, 1284.13 $[M-L]^+$. FAB$^+$-MS (*m*/*z*): 1572 ($[M\text{-phen}]^+$, 16%). IR (CsI, cm^{-1}): 1140, 1187 (ν_{PO}), 423 ($\nu_{Er\text{-}X}$, X = O,N). UV−vis (10^{-5} *M*, CH_2Cl_2, nm/ ε M^{-1} cm^{-1}): λ_1 267 (84180), λ_2 274 (62210), λ_3 294 (21980). μ_{eff} (20 °C) = 9.04 μ_B.

X-ray Structure Determination. Suitable single crystals of solvate **1**−**5** compounds were grown by slow evaporation from a DMSO/Methanol mixture. They were collected using the program SMART[34] on a Bruker APEX CCD diffractometer with monochromatized Mo Kα radiation (λ = 0.71073 Å). Cell refinement and data reduction were carried out with the use of the program SAINT.[34] The program SADABS[35] was employed to make incident beam and decay corrections in the SAINT-Plus version 6.23c suite.[35] Then, the structures were solved by direct methods with the program SHELXS[36] and refined by full-matrix least-squares techniques with SHELXL.[36] Hydrogen atoms attached to C atoms were generated in calculated positions and constrained with the use of a riding model, while those bonded to water solvent molecules were located on difference Fourier maps at advanced stages and their positional parameters were refined. The final models involved anisotropic displacement parameters for all non-hydrogen atoms. Some of the phenyl rings in **1** and the coordinated and uncoordinated solvent molecules display some degree of disorder. The disorder was modeled splitting the groups into two orientations and the refinements were achieved using combination of the SIMU, DELU, and SAME restraints in SHELXL.[36] In addition, structures **2**−**5** display some degree of racemic twin as can be judged by the refined values of the Flack's parameter. Selected crystallographic data are given in Table 1.

Results and Discussion

Compounds **1**−**8** were obtained by the reaction of the appropriate $LnCl_3\cdot nH_2O$ with three molar equivalents of the potassium salt of the ligand (KL) in THF. KL was not very soluble, but once the lanthanide chloride was added, the solution became clear. This solution was stirred until the desired complex precipitated. For the $LnL_3(phen)\cdot nH_2O$ series (**9**−**16**), 1,10-phenanthroline (a molar equivalent) was added as soon as the clear solution was obtained. The products were recovered by extracting the solvent and filtering the solid suspended in water. The yields of $LnL_3\cdot nH_2O$ were around 80%, while those of $LnL_3(phen)\cdot nH_2O$ dropped

(34) *SMART* (*Version 5.625*), *SAINT-Plus* (*Version 6.23C*); Bruker-AXS: Madison, WI, 2000.

(35) Sheldrick, G. M. *SADABS*, Version 2004-1; University of Göttingen: Göttingen, Germany; Bruker-AXS: Madison, WI, 2005.

(36) Sheldrick, G. M. *Acta Crystallogr.* **2008**, *A64*, 112.

Table 2. UV−vis Absorption and Luminescence data of **6**, **7**, **11**, **14**, **15**

complex	λ/nm (ε/ M^{-1} cm^{-1})	quantum yield Φ_F/%	λ_{exc}/nm	λ_{det}/nm	luminescence τ/ms
$NdL_3(phen)\cdot 5H_2O$ (**11**)	267 (74780) 274 (78840) 294 (27820)	0.50	267	1076	1.25 ± 0.0112
$EuL_3\cdot 6H_2O$ (**6**)	267 (29450) 274 (21900)	0.76	267	613	2.16 ± 0.0007
$EuL_3(phen)\cdot 2H_2O$ (**14**)	267 (105710) 274 (93720) 294 (26870)	0.84	267	613	1.58 ± 0.0005
$TbL_3\cdot 4H_2O$ (**7**)	267 (24180) 274 (32280)	0.89	267	548	2.69 ± 0.0006
$TbL_3(phen)\cdot 4H_2O$ (**15**)	267 (66510) 274 (57520) 294 (16350)	1.45	267	548	1.75 ± 0.0057

to 70−35%. The solubility was quite different between both series. While the LnL_3(phen) complexes were very soluble in THF, CH_2Cl_2, CH_3CN, and DMSO, the LnL_3 compounds were clearly less soluble in CH_2Cl_2, CH_3CN, and only partially soluble in THF. The exposure of the $EuL_3(phen)\cdot 2H_2O$ (**14**) and $TbL_3(phen)\cdot 4H_2O$ (**15**) powders to long wave UV light yielded strong red and green emissions, which are characteristic of the corresponding ions.

Magnetic Moments. The experimental μ_{eff} values of all Ln complexes show a small deviation from the theoretical values predicted by eq 1. These deviations of μ_{eff} values suggest that the *f* electrons of the metal Ln do not interact directly with the ligands; they are well shielded by the 5s and 5p electrons.[37]

$$\mu_{eff} = g\sqrt{[J(J+1)]} \quad (1)$$

Infrared and Raman Spectroscopy. The vibrational spectra of the compounds show bands of aromatic νCH and νCC, νCN vibrations around 3060 and 1580 cm^{-1}, respectively. The phosphoryl stretching mode exhibits a lowering in relation to that at 1201 cm^{-1} for the free ligand. They are observed as single intense and broad ν(PO) bands around 1134−1155 cm^{-1} for $LnL_3\cdot nH_2O$ and 1149−1154 cm^{-1} for $LnL_3(phen)\cdot nH_2O$. Both of them show ill-defined shoulders at higher frequency (around 1185 cm^{-1}) that can be attributed to a non-coordinate PO group, suggesting an unsymmetric ligand coordination mode, with the N,O-chelate holding a "free" phosphoryl group. In addition, both series of complexes exhibit a couple of new bands in the far IR, which might be attributed to νLn-O and/or νLn-N vibrations.[38,39]

Raman spectra recorded with the He−Ne laser line (632.8 nm, 1.96 eV) revealed some important signals for the $LnL_3\cdot nH_2O$ series, mainly attributed to vibration modes of the ligand, except for the compounds where a dominant photoluminescence effect is observed [Sm (**4**), Eu (**6**), and Er (**8**)]. Thus, bands assigned to C−H stretching and aromatic ring vibrations are observed at 3066 and 1600−1010 cm^{-1}, respectively;[40] representative spectra have been assembled in Supporting Information, Figure S1. As for the $LnL_3(phen)\cdot nH_2O$ series, the signals observed for both free ligands are obscured by a strong photoluminescence; interestingly, however, only a set of three bands of the triazolate ligand or the most intense of them (at ca. 1000 cm^{-1}) outstands the PL band for the La, Ce, Nd, Sm, Gd and Er complexes, while the most intense band of the phenanthroline ligand (at ca. 1400 cm^{-1}) is not observed; the spectrum of $LaL_3(phen)\cdot 3H_2O$ (**9**) is shown in Supporting Information, Figure S1 as example. This important change on going from the free phenanthroline ligand to the $LnL_3(phen)\cdot nH_2O$ series is indicative of the coordination of the former to the different metal ions.

UV−vis and Photoluminescence Spectroscopy. UV-vis absorption spectra in CH_2Cl_2 of both series of complexes and the ligand (**L**) reveal absorption bands at λ_{max} = 267 and 274 nm. A third band appears in the $LnL_3(phen)\cdot nH_2O$ series at 294 nm, attributed to the coordinated 1,10-phenanthroline (294 nm). The molar absorption coefficient (ε) at 267 and 274 nm increases considerably when incorporating the auxiliary ligand (see Table 2). Excitation spectra of the Eu(II), Tb(III) complexes (**6**, **7**, **14**, **15**) and $NdL_3(phen)\cdot 5H_2O$ (**11**) show a slightly low energy shifted absorption in relation to their absorption spectra. This is indicative of an energy transfer from the ligand to the metal as a result of an antenna effect.[5,20] Upon excitation at 267 nm, $EuL_3\cdot 6H_2O$ (**6**) and $EuL_3(phen)\cdot 2H_2O$ (**14**) exhibit strong emission bands corresponding to characteristic transitions of the trivalent europium ion: $^5D_0 \rightarrow {}^7F_1$ (590 nm), $^5D_0 \rightarrow {}^7F_2$ (613 nm), $^5D_0 \rightarrow {}^7F_3$ (654 nm), $^5D_0 \rightarrow {}^7F_4$ (690 nm), $^5D_0 \rightarrow {}^7F_5$ (700 nm) (Figure 1a). The intensity of the emission bands in **14** is higher in relation to that observed in **6**. When excited at 267 nm, **7** ($TbL_3\cdot 4H_2O$) and **15** ($TbL_3(phen)\cdot 4H_2O$) exhibit emission bands attributed to the electronic transitions of Tb(III): $^5D_4 \rightarrow {}^7F_6$ (490 nm), $^5D_4 \rightarrow {}^7F_5$ (548 nm), $^5D_4 \rightarrow {}^7F_4$ (584 nm), $^5D_4 \rightarrow {}^7F_3$ (618 nm) (Figure 1b). Similarly to the europium complexes, the intensity of these emission bands is higher in $TbL_3(phen)\cdot 4H_2O$. In addition, we have observed comparable bright luminescence in water suspension for the four Eu(III) and Tb(III) complexes, which is an important feature for their potential applications. Finally, when $NdL_3(phen)\cdot 5H_2O$ (**11**) was also excited at 267 nm, it showed characteristic emission bands in the near-infrared region, attributed to the luminescent transitions $^4F_{3/2} \rightarrow {}^4F_{9/2}$ (872 nm) and $^4F_{3/2} \rightarrow {}^4F_{11/2}$ (1073 nm) (Figure 1c).[5] No emission was detected in the wavelength

(37) Cotton, S. *Lanthanide and Actinide Chemistry*; John Wiley & Sons Ltd: Chichester, England, 2006.
(38) Pretsch, E.; Simon, W.; Seibl, J.; Clerc, T. *Tables of Spectral Data for Structure Determination of Organic Compounds*; Springer-Verlag: Berlin, 1989.
(39) Emsley, J.; Hall, D. *Chemistry of phosphorous*; Harper Collins Publishers: London, 1976.
(40) Lin-Vien, D.; Colthup, N. B.; Fateley, W. G.; Grasselli, J. G. *The Handbook of Infrared and Raman Characteristic Frequencies of Organic Molecules*; Academic Press: San Diego, 1991.

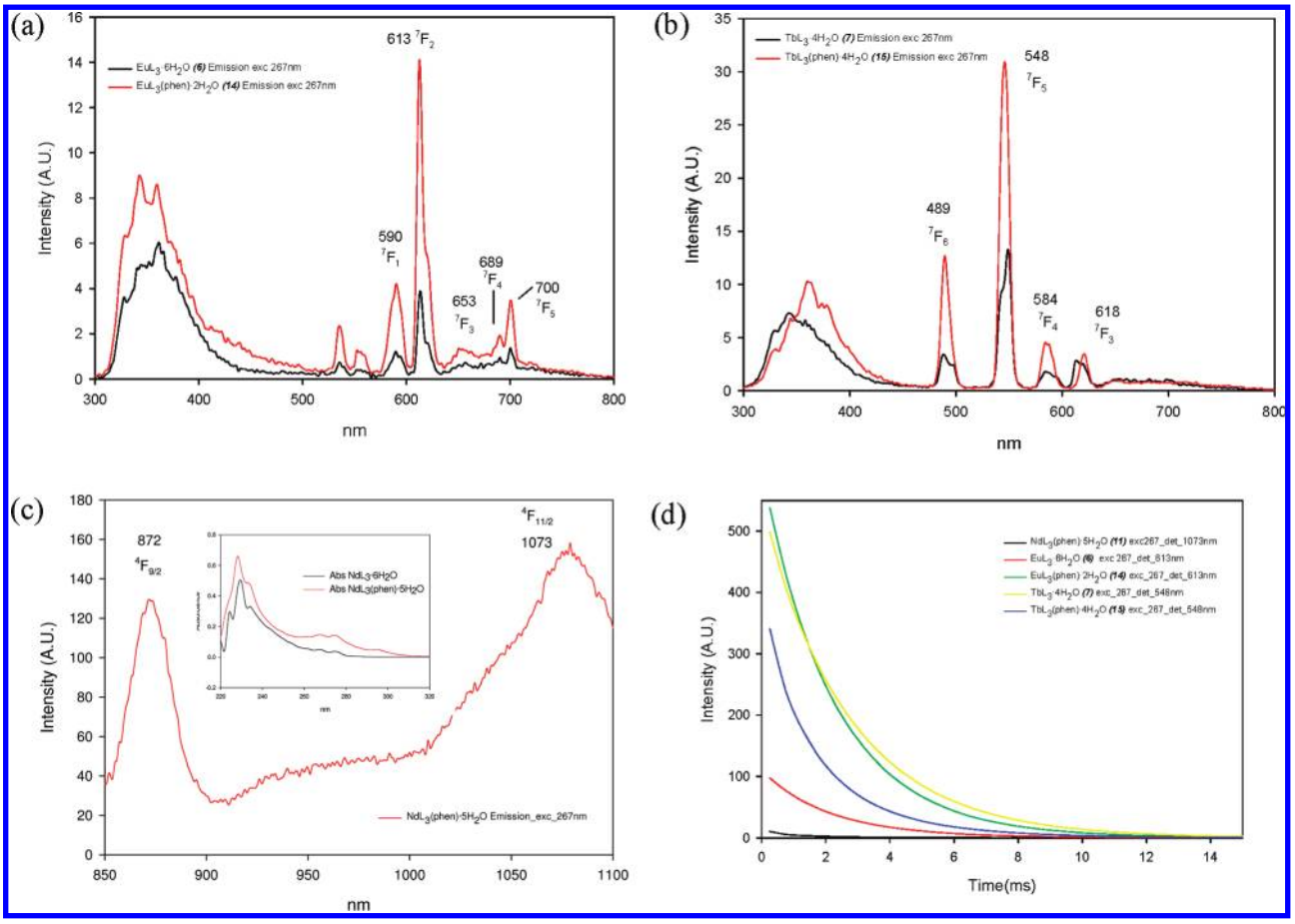

Figure 1. Emission spectra of $LnL_3 \cdot nH_2O$ and $LnL_3(phen) \cdot nH_2O$: (**a**) **Ln** = Eu (**6** and **14**), (**b**) Ln = Tb (**7** and **15**); (**c**) Emission spectrum of $NdL_3(phen) \cdot 5H_2O$ (**11**) and (*as inset*) absorption spectra of both Nd complexes (**3** and **11**), (**d**) Luminescence lifetimes upon excitation at 267 nm for **11**, detecting at 1073 nm; **6** and **14**, detecting at 613 nm; **7** and **15**, detecting at 548 nm.

range covered by our spectrometer for $NdL_3 \cdot 4H_2O$ (**3**) or the other complexes studied. Emission quantum yields (Φ_F) and luminescence lifetimes were also obtained (Table 2). In general, terbium complexes **7** and **15** are the ones that exhibit the higher quantum yields, 0.89 and 1.45, respectively. The higher quantum yields upon excitation at 267 nm of the complexes containing 1,10-phenantroline should be highlighted. It proves that its incorporation promotes the luminescence of these complexes. On the other hand, the luminescence lifetimes (τ) of the complexes with phenanthroline are shorter than those of the $LnL_3 \cdot nH_2O$ series. The complexes studied exhibit monoexponential decay curves, indicating the presence of single species in solution. In accordance with the quantum yields, compounds **7** (2.69 ms) and **15** (1.75 ms) have the longest luminescence lifetimes, while the neodymium complex **11** exhibits the fastest luminescence decay. Similar lanthanide complexes[23] present considerably shorter luminescence lifetimes (μs) than those reported in this work (ms).

Mass Spectrometry. The FAB mass spectra of both series of complexes exhibit signals for the molecular ion $[M+1]^+$ (relative intensities 2−78%); the corresponding electrospray ionization (ESI) mass spectra show signals of the molecular ion $[M+1]^+$ and $[M+2H_2O \pm H]^+$ as well. In the $LnL_3(phen) \cdot nH_2O$ series the fragments attributed to $[M\text{-phen}]^+$ and $[M - L - H]^+$ can also be identified. All of the observed signals exhibited the expected characteristic isotopic distribution patterns. More peak assignments are given in the Experimental Section.

Thermogravimetric Analysis and Simultaneous Differential Thermal Analysis. TGA/SDTA analyses were performed for both types of complexes and the starting materials. The observed weight loss patterns are very similar within each series. The first weight loss, from 40 to 140 °C, corresponds to the loss of two to six guest water molecules, depending on the complex. A second weight loss, from 180 to 280 °C, in both $LnL_3 \cdot nH_2O$ and $LnL_3(phen) \cdot nH_2O$ series with Ln = La, Sm, Gd and Er, corresponds to the loss of one water molecule of one of the two following types: non-coordinate water tightly hydrogen bonded to a "free" P═O group, or metal coordinated water. The absence of the fusion process of 1,10-phenanthroline at 100 °C in the $LnL_3(phen) \cdot nH_2O$ series confirms its coordination to the metal center. In addition, both series of complexes showed decomposition processes near 400 °C (see Experimental Section).

NMR Spectroscopy. Despite the paramagnetic properties of some of the synthesized complexes, ^1H and ^{31}P NMR spectra could be obtained for most of them in DMSO-d_6 and $CDCl_3$-d_1. The ^1H NMR spectra of the $LnL_3 \cdot nH_2O$ series present signals between 7 and 8 ppm, thus confirming the presence of the aromatic rings of the ligand. The $LnL_3(phen) \cdot nH_2O$ series also exhibits signals whose integration corresponds to the 12 aromatic rings of 3 coordinated ligands L^-, at 6.5−7.5 ppm, as well as resolved signals of one coordinated molecule of 1,10-phenanthroline within the 7.5−9 ppm range, low field

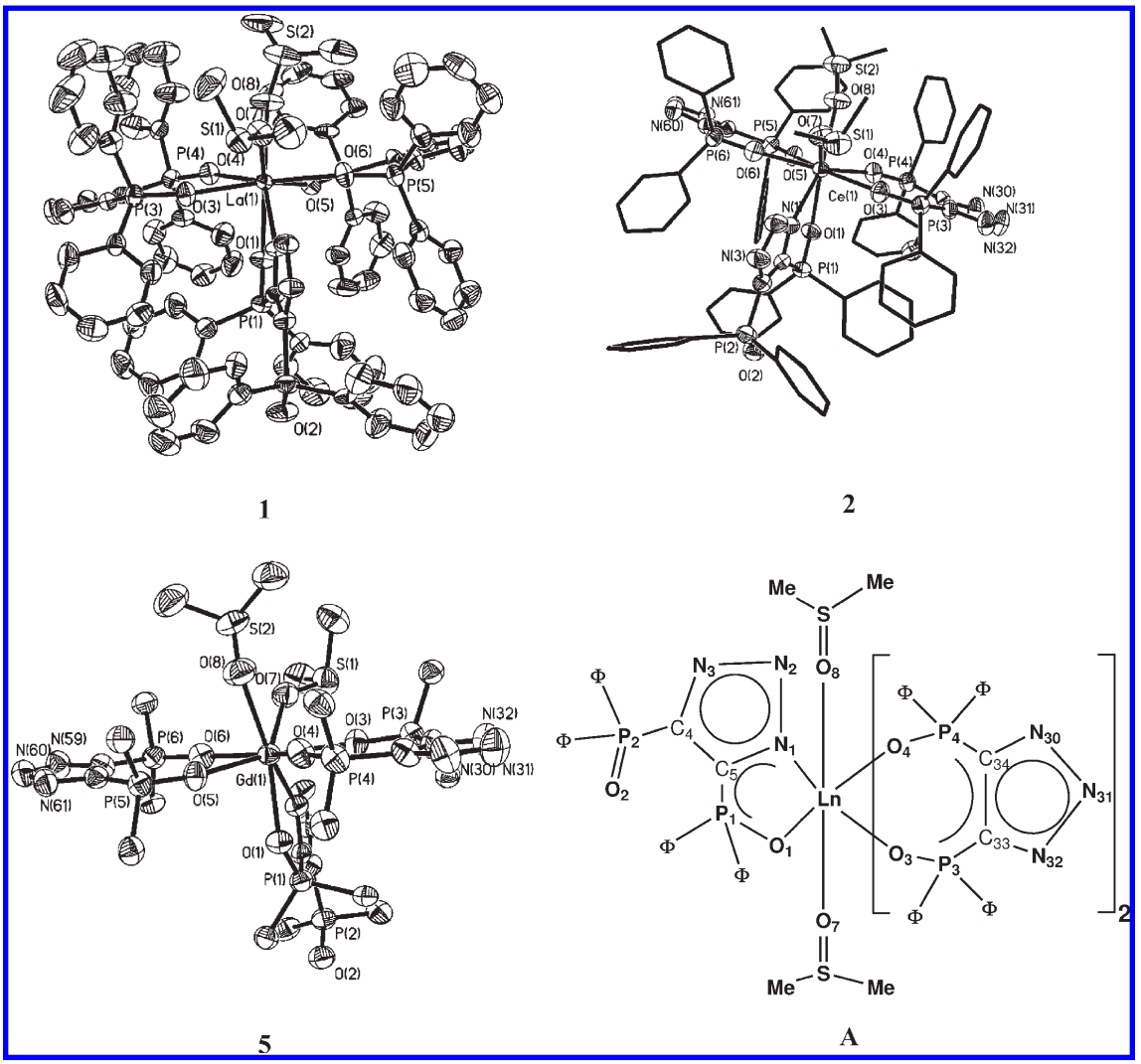

Figure 2. Molecular structure of **1** (La), **2** (Ce), **5**(Gd) (guest solvent were omitted and phenyl groups were modified for clarity), and atomic labeling scheme (**A**).

shifted in relation to non-coordinate phenanthroline in DMSO-d_6. The paramagnetic properties of most of the complexes caused a broadening of these signals. The ^{31}P NMR spectra of the $LnL_3 \cdot nH_2O$ complexes exhibit two signals: one, around 17 ppm, and the other at either lower or higher field depending on the lanthanide ion; thus, NdL_3 and CeL_3 show the lowest field shift at 104 and 50 ppm, respectively, while in LaL_3 and SmL_3 this signal appears at 26 ppm. The Eu and Tb complexes exhibit high field shifts at −70 and −160 ppm, respectively. The $LnL_3(phen) \cdot nH_2O$ series also shows two signals, one, around 17 ppm too, and a second signal, shifted to lower field values, between 25 and 100 ppm for **9**−**12**. The lowest field shift was also found for the $NdL_3(phen)$ complex (100 ppm). In the case of Eu and Tb complexes (**14** and **15**), they exhibit high field shifts (−83 and −153 ppm, respectively). These two signals indicate that the observed unsymmetric coordination mode of the ligands to the metal in the solid state (see Figure 2A) is also present in solution. Thus, the signal around 17 ppm was assigned to the "free" phosphoryl group from the O,N-coordinate ligand (free ligand at 21.4 ppm in DMSO-d_6), while the shifted resonance corresponds to the phosphorus attached to the coordinate O atoms. ^{31}P NMR experiments at higher temperatures were performed in CD_2Cl_2-d_2 and showed a gradual collapse of the two signals. For instance, at 338 K, $LaL_3(phen) \cdot 3H_2O$ exhibits only one broad signal around 24 ppm, indicating the existence of a fast dynamic equilibrium between two different ligand coordination modes on the ^{31}P NMR time scale.

X-ray Structures. The crystal structures of the solvate $[LnL_3]$ (Ln(III) = La (**1**), Ce (**2**), Nd (**3**), Sm (**4**), and Gd(**5**)) consisted of discrete $[LnL_3(DMSO)_2] \cdot 2H_2O$ molecules. The gadolinium complex presented in addition, a molecule of methanol as crystallization solvent, while the lanthanum derivative contained 1.5 DMSO molecules per $[LnL_3(DMSO)_2]$ unit. The molecular structure and atomic labeling scheme of $[LaL_3(DMSO)_2] \cdot 3/2DMSO$, $[CeL_3(DMSO)_2] \cdot 2H_2O$, and $[GdL_3(DMSO)_2] \cdot 2H_2O \cdot MeOH$ are depicted in Figure 2. In all complexes, two ligands are bonded symmetrically to the lanthanide atom, forming seven-chelate rings, while the third one is unsymmetrically attached to the metal through one oxygen atom and the N(1) of the triazole, giving a five-chelate ring. Therefore, the coordination number of the lanthanide atom is eight, comprising two O,O-coordinate ligands ($\mathbf{L}^-$), one O,N-coordinate ligand, and two oxygen atoms

from two coordinate DMSO molecules (Figure 2). The coordination environment may be best described as a distorted trigonal dodecahedron in which the two DMSO molecules occupy adjacent positions. This situation led to the idea of including an auxiliary ligand, to exclude water or any solvent from the lanthanide coordination sphere, since their presence could induce the quenching of luminescence.

On the other hand, it is interesting to note that the structure of $LaL_3(DMSO)_2]\cdot 1.5DMSO$ described above, with two symmetric and one unsymmetric coordinate ligands, is different from that sketched by Trofimenko for $LaL_3(DMF)_2$, in which the three ligands were reported to exhibit an O,O-bidentate coordination mode.[32]

The lanthanide contraction is apparent in the Ln−O bond lengths: as expected, a subtle lessening in Ln−X (X = O, N) bond lengths from La (av. 2.483 Å) to Gd (av. 2.38 Å) is observed. The Ln−O and P−O bond lengths are within the interval of 2.501(4) to 2.359(5) Å (Ln−O) and 1.486(5) to 1.509(5) Å (P−O), respectively. These bonds are comparable with those reported for lanthanide derivatives containing P, O-based ligands, such as $[Nd(N(Ph_2PO)_2))_3]$,[23] $[Ln(CH_2(Ph_2PO)_2)_2(NO_3)_3]$,[25] and $[La(Ph_3PO)_4(NO_3)_3]\cdot Me_2CO$.[30] It is noteworthy that the Ln−O(DMSO) bond distances (av. 2.466 Å) are also quite similar to Ln−O bond lengths (av. 2.422 Å) with the coordinated phosphoryl ligand. The O−Ln−O bite angles (from 69.4° to 70.8°) are smaller than those in related $[UO_2L_2(DMF)]$[32] or in lanthanide (La, Ce, Nd, and Gd) complexes containing the $CH_2(Ph_2PO)_2$ ligand.[25]

The non-coordinate phosphoryl group exhibits P−O bond lengths within the interval of those where there is oxygen to metal coordination. However, it is remarkable that the "free" P−O bond distances (1.465(5) to 1.485(5) Å) are still lengthened in comparison to trimethylphosphine oxide (1.44 Å)[41] and phosphorus pentoxide (1.43 Å).[42] This may be accounted for by the influence of O−H···O=P hydrogen bonding established between the "free" phosphoryl group and a guest water molecule. The P=O bond distances found (av. 1.473 Å) are also comparable with those observed in reported complexes containing the same oxygen ligand with a non-coordinate P−O group, that is, $[Me_2In(O,N,N\text{-}L]_2$ (1.480(6) Å)[33] and $[CoL_2py_2]\cdot 2py$ (1.497(2) Å).[32] The O−H···O=P hydrogen bond distances between 2.773 and 2.793 Å are well below the sum of van der Waals radii for oxygen. Such O−H···O=P distances are comparable with reported H-bonding.[25,43] There is also O−H···O bonding between the water molecules attached to the P−O group and another guest water molecule (O−O 2.952 to 2.974 Å), as well as some longer O−H···N interactions.

(41) Wang, H. K. *Acta Chem. Scand.* **1965**, *19*, 879.
(42) Chandrasekhar, V.; Azhakar, R. *CrystEngComm*. **2005**, *7*, 346.
(43) Chandrasekhar, V.; Azhakar, R.; Bickley, J. F.; Steiner, A. *Cryst. Growth Des*. **2006**, *6*, 910.

Conclusion

We have introduced the 4,5-bis(diphenyl)phosphoranyl-1,2,3-triazolate ($\mathbf{L}^-$) as a successful "antenna" ligand for sensitizing both europium and terbium emission. The coordination of 1,10-phenanthroline leads to an increase in the quantum yields of the metal-centered emission of the complexes, clearly observed for Nd, Eu, and Tb compounds (**11**, **14**, **15**). In the solid state, the complexes also show strong photoluminescence bands, which are enhanced by the presence of the phenanthroline ligand as well; in this case, the europium and terbium complexes show the stronger emissions too. The crystal structures of the $LnL_3\cdot nH_2O$ solvates show eight-coordinated lanthanide ions, with the ligands exhibiting two different coordination modes, symmetrical O,O-bidentated and unsymmetrical O,N-bidentated, as well as two neighboring solvent molecules. The ligand coordination behavior is maintained also in solution, as shown by two distinct resonances in the $^{31}P\{^1H\}$ NMR spectra of all the reported compounds. The observed coordination arrangement allowed the replacement of coordinate solvent molecules with 1,10-phenanthroline, which acts as an auxiliary ligand.

Acknowledgment. This research was supported by CONACyT (Project Grant 40620-F) and UNAM-DGAPA (Project Grant IN212808). We thank M. C. Ma. de las Nieves Zavala Segovia, Q. Pedro Navarro, I.Q. María del Carmen Delgado Cruz, Ing. Francisco Rodríguez Melgarejo, and Q. Eréndira García Ríos for their work in recording ESI-MS, Photoluminescence (in solution), TGA/SDTA and Raman spectra, and the Elemental Analyses.

Supporting Information Available: CIF files of the crystal structures. Table S1 containing selected bond lengths [Å] and bond angles [deg] of **1**·(3.5 DMSO), **2**−**4**·(2DMSO, $2H_2O$), and **5**·(2DMSO, $2H_2O$, MeOH). Figure S1 showing representative Raman spectra for both $LnL_3\cdot nH_2O$ and $LnL_3(phen)\cdot nH_2O$ series. This material is available free of charge via the Internet at http://pubs.acs.org.